

See discussions, stats, and author profiles for this publication at: <https://www.researchgate.net/publication/233847556>

Characterization of Triplet State of Hybridization-Sensitive DNA Probe by Using Fluorescence Correlation Spectroscopy.

ARTICLE in THE JOURNAL OF PHYSICAL CHEMISTRY A · DECEMBER 2012

Impact Factor: 2.69 · DOI: 10.1021/jp307018k · Source: PubMed

CITATIONS

4

READS

27

6 AUTHORS, INCLUDING:



Shin Hyosup

Samsung

3 PUBLICATIONS 5 CITATIONS

SEE PROFILE



Sokwon Kim

University of Ulsan

462 PUBLICATIONS 11,630 CITATIONS

SEE PROFILE



Chan-Gi Pack

ASAN Institute for Life Sciences, ASAN Medical...

43 PUBLICATIONS 877 CITATIONS

SEE PROFILE

Characterization of the Triplet State of Hybridization-Sensitive DNA Probe by Using Fluorescence Correlation Spectroscopy

Hyo-Sup Shin,[†] Akimitsu Okamoto,[‡] Yasushi Sako,[§] Sok Won Kim,^{||} Soo Yong Kim,^{*,†} and Chan-Gi Pack^{*,§}

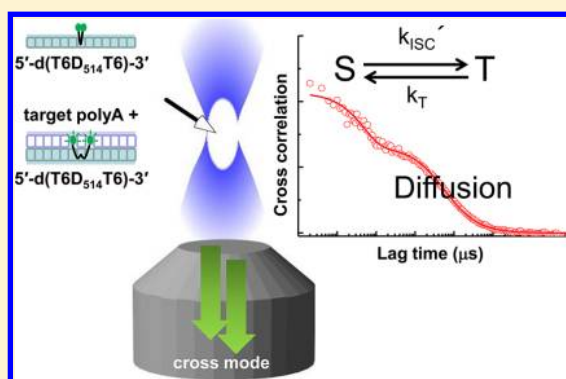
[†]Department of Physics, Korea Advanced Institute of Science and Technology, Daejeon 305-701, South Korea

[‡]Research Center for Advanced Science and Technology (RCAST), The University of Tokyo, 4-6-1 Komaba, Meguro-ku, Tokyo 153-8904, Japan

[§]RIKEN Advanced Science Institute, 2-1 Hirosawa, Wako-shi, Saitama 351-0198, Japan

^{||}Department of Physics, University of Ulsan, Ulsan 680-749, South Korea

ABSTRACT: The nonradiative relaxation mechanism of the newly synthesized hybridized-sensitive DNA probe has not been fully understood until now. In this study, the transient dark state of the probe, which is a double fluorescent dye attached to a specific DNA sequence, was investigated using a fluorescence correlation spectroscopy (FCS). The transient dark state was measured in various solvents that are known to affect the intersystem crossing or photoisomerization of the DNA probe. On the basis of the experimental results, a simplified two energy state model of the probe was constructed, and this model provides an insight into the nonradiative relaxation mechanism of the fluorophore and the applications for DNA and RNA detection. The transient dark state that was measured in a time scale of a few microseconds is a triplet state and is related to photoisomerization, viscosity, oxygen concentration, and hybridization, all of which are important parameters for cellular microscopy. The transient dark state in a time scale of a sub-microseconds is sensitively changed after the addition of target DNA. The characterization can improve the probe's capability to identify target DNA/RNA by using FCS since the triplet state that occurred after hybridization is distinctive in the time scale with that occurred before hybridization.



INTRODUCTION

A hybridized sensitive DNA/RNA probe (Figure 1A), which was developed for RNA visualization in live cell, is strongly selective for the target DNA/RNA sequence because the base sequence of the probe is designed to be complementary to the sequence of the target DNA/RNA.^{1–3} The brightness of the fluorophore attached to the middle of the probe is dramatically changed before and after the hybridization of the probe with target. Prior to the hybridization with the target, the fluorophores exist as two conformations, i.e., monomeric and dimeric forms, in an aqueous solution. The conformation changes to a single monomeric form after the hybridization with the target DNA because the fluorophores are intercalated into the DNA through the molecular interaction between the bases and them. The probe produces a bright emission when it is bound to the target DNA and a dim emission when it is not. Because of its good selectivity for a specific target, the probe can be properly used for DNA tracking/quantification in vitro or visualization/imaging of mRNA/miRNA in a living cell, and so on.⁴ However, the probe emits relatively strong fluorescence intensity without the presence of target molecules because two thiazole oranges of the probe are located in close proximity,

which results in strong tendency of dye aggregation in polar solvent.² Therefore, the emission difference of the probe before and after the hybridization reaction is significantly small compared with that of the conventional thiazole orange dye. This property makes the intensity-based DNA/RNA detection difficult in live cell experiments. In addition, the triplet state of the fluorophore (double thiazole orange; D₅₁₄) in the hybridized sensitive DNA probe was not characterized while the photoisomerization of the probe is well established in previous studies. Since the triplet state relaxation is strongly affected by solvent viscosity and target concentration, which are now known to be changed in live cells at various compartments, photophysical and photochemical characterization of the probe in addition to molecular concentration, diffusion, and interaction parameters by FCS/FCCS analysis will be complementary and helpful for a better application in live cells as well as the visualization.^{3–5}

Received: July 16, 2012

Revised: November 29, 2012

Published: December 4, 2012

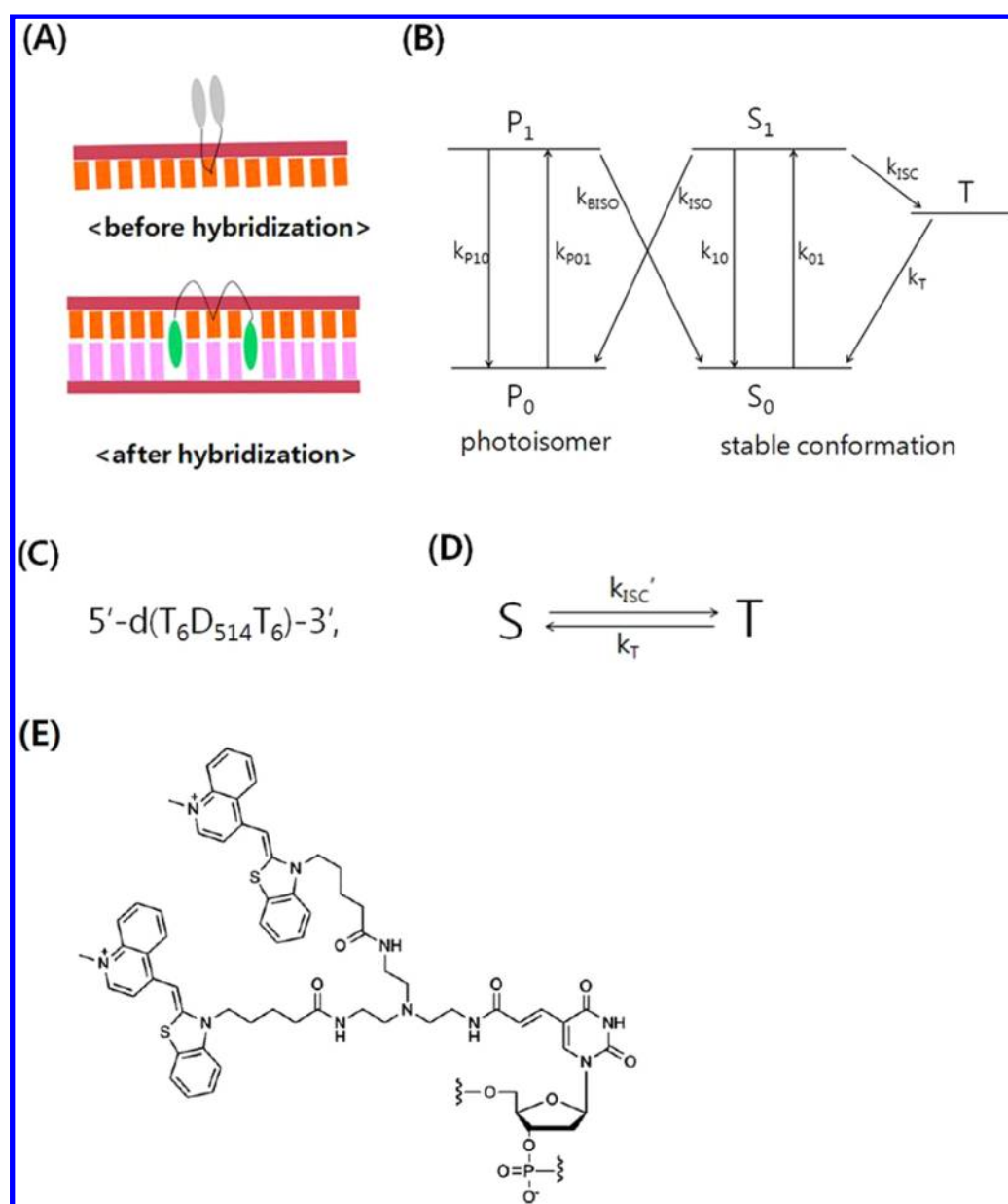


Figure 1. (A) Schematic representation of a dye conformation of the probe, D_{514} , before and after hybridization with target. (B) S_0 , S_1 , and T_1 denote the ground singlet, first excited singlet, and triplet states, respectively, of the thermodynamically stable conformation of the dye. P_0 and P_1 are the ground singlet and first excited singlet states of photoisomer. (C) Schematic representation of base sequence and the dimeric fluorophore, D_{514} , of the probe. (D) Two energy states model. (E) Chemical structure of D_{514} .

The photoinduced isomerization and intersystem crossing are known as the dominant process of the nonradiative deactivation of the singlet excited state of cyanine dyes.⁶ The hindrance of torsional rotation of the methine bridge is primarily determined by dye conformation and solvent viscosity because they influence the trans–cis isomerization rate of the probe. Cyanine dye with a dimeric form or with a substituent in the meso-position of the polymethine bridge is known to have a relatively strong deactivation pathway through the intersystem crossing.⁸ A smaller energy difference between the singlet and triplet energy states and decrease of k_{10} or k_{iso} are believed to be responsible for the increase of the triplet state population.⁹ Population of triplet state might be relatively sensitive to the change of environment compared to the population of the isomer state. In the case of the isomer state, the change of its population is reduced because both of the isomerization and

back-isomerization rates are increased or decreased simultaneously according to the factors that influence the rotation of the methine bridge. For widely used conventional cyanine dyes such as Cy5, the photochemical properties are minutely investigated in various conditions using FCS.⁶ For Cy5, a simplified state model was adopted, and the rate constants related to isomerization were obtained using a global fitting analysis. It was reported that the transient isomerization state of Cy5 can be used to analyze DNA hybridization.⁷ In this previous investigation on cyanine dye, photoisomerization appeared as a dominant transient dark state in a few microseconds time scale. Since the dark state fraction caused by photoisomerization is determined by isomerization and back-isomerization simultaneously, it may be relatively insensitive to the change of hindrance of the methine bridge.

In this study, we focus on the transient dark state of the newly developed DNA probe, which was investigated using FCS and identified as a triplet state. To our knowledge, triplet state was not clearly discernible in previous FCS experiments for cyanine dyes because intersystem crossing is an event rarely happening in usual aqueous solvents without intersystem crossing enhancer, i.e., potassium iodide. Larger population of triplet state of the DNA probe can be ascribed to a sufficiently smaller triplet relaxation rate compared to the intersystem crossing rate.^{10,11} We show that the triplet dark state of the probe exhibited characteristic and sensible behaviors under the specific chemical environments in aqueous solutions. Interestingly, this result suggests that the photochemical information can be used to understand the chemical microenvironment of a live cell through the parameters if it is specifically influenced by the local cellular viscosity, oxygen concentration, and density of target DNA/RNAs, all of which is hardly understood by conventional methods of imaging/visualization.

■ EXPERIMENTAL SECTION

The oligodeoxyribonucleotide strands labeled with thiazole oranges, 5'-d(T₆D₅₁₄T₆)-3', were investigated and prepared according to the protocols described in ref 12.

The fluorescence cross-correlation of the solution sample was measured using a ConfoCor 3 built on LSM710 confocal microscopy (Carl Zeiss). An argon ion laser with a 514 nm wavelength was focused by a C-Achromat 40 × 1.2 water immersion objective lens in order to excite the samples. An OPHIR power meter (PD300-SH) was used to measure the incident laser power at the sample position. The average laser power at the sample was, unless otherwise specified, adjusted to 80% laser transmission with a 100% acoustic-optical tunable filter. The laser power with 80% transmission was 190 μW (154 kW/cm²) at the output of an objective lens. The measured power has a direct proportional relationship with laser transmission rate. In order to exclude after-pulsing effects from the correlation functions, the fluorescence emitted from the sample passed through a 50/50 beam splitter and was equally divided into two APD detectors, and cross-correlation analyses were performed. The pinhole radius was fixed to 1 AU (Airy Unit, 36 μm) for 514 nm. Two band-pass filters of 530–610 nm were placed in front of each detector in order to discriminate the fluorescence from elastic scattered laser light. All measurements were performed with time resolution of 50 ns. The probe concentration was fixed to 5 nM and 500 mM NaCl concentration. Target DNA was not added to the samples unless otherwise specified. The samples were loaded on the Lab-Tek chambered coverglass with eight wells (Nalge Nunc International). Unless otherwise specified, the viscosity of the solvents was fixed to 2.5 cP by mixing water with glycerine. A control experiment was performed with Rh6G.

The fluorescence quantum yield of the samples was measured using an Infinite M200 microplate reader (Infinite200 PRO series, Tecan Group Ltd.). The temperature of the samples was fixed at 20 °C using the built-in temperature controller of the spectrometer. The probe concentration was fixed to 0.5 μM, and the target was 1 μM. The samples were reserved in 5 °C for more than two days in order to complete a hybridization of the probe with the target. The absorption spectrum was corrected using the background signal from the solvent. The ionic strengths of all samples were fixed with 100 mM of NaCl throughout the measurements, unless otherwise specified. The fluorescence measurements were performed at a

470 nm excitation wavelength. The fluorescence quantum yield for the samples was determined by comparison with coumarin343 in ethanol ($\Phi_R = 0.63$).

All samples were prepared with ACS reagents (Sigma-Aldrich Corp.) and deionized water (18 MΩ resistivity, Milli-Q, Millipore) without further purification. The solvent viscosity was altered through glycerine additions. The reaction process was performed at room temperature for more than 24 h in order to complete a reaction of the samples.

■ RESULTS AND DISCUSSION

Figure 1B shows the schematic energy states normally used to explain the photophysical and photochemical behaviors of cyanine dye.⁶ The S_0 , S_1 , and T_1 denote the ground singlet, first excited singlet, and triplet states, respectively, of the thermodynamically stable conformation of the dye. P_0 and P_1 are the ground singlet and first excited singlet states of the photoisomerized form induced by the rotational motion around the methine bridge.⁶ The photoisomer returns to a thermodynamically stable state, S_0 , after the electron is excited into a singlet excited state of the photoisomer, P_1 . The direct back isomerization from the P_0 state to the S_0 state is neglected in this study since it may take place in a time scale of a few milliseconds.¹² It is assumed that the dye emission is too weak to contribute to the experimental results when it is in a triplet or photoisomerized state.⁶ The triplet state of the photoisomer can be ignored since the singlet excited state of the photoisomer is known to be mostly deactivated through internal conversion.¹³ This schematic description may also be assumed to be applied to the dimer conformation of the dye, D₅₁₄. If two thiazole oranges are aggregated in a parallel way, the S_1 state is split into two energy levels with an energy gap of 1000–2500 cm⁻¹.¹⁴ As shown in our previous study,² the upper energy level is corresponding to the in-phase dipole interaction, while the lower energy level is corresponding to the out-of-phase dipole interaction. The absorption occurs mostly in the upper energy level of the S_1 state because it is an allowed state due to the dipole transition. The excited electron is nonradiatively deactivated to the lower energy level of the S_1 state; then, it is deactivated to the S_0 state with a radiative or nonradiative pathway. These two states, the upper and lower energy levels, may be simplified as a single S_1 state in this model. The electrons excited to the S_1 state were nonradiatively deactivated primarily through the intersystem crossing (k_{isc}) and photoinduced isomerization (k_{iso}). The excited singlet state of the photoisomer can be back-isomerized to the ground singlet state (k_{biso}). The ground and excited states of the photoisomer can be simplified to one state by adopting an effective kinetic rate (k'_{biso}), which is defined by eq 1, as follows.

$$k'_{biso} = \frac{k_{p01}}{k_{p01} + k_{p10}} k_{biso} \quad (1)$$

where k_{p01} and k_{p10} are the excitation and de-excitation rates, respectively, of the electron in the photoisomer. Effective back-isomerization rate refers to the corrected back-isomerization rate based on the population of the excited singlet state of the photoisomer. The electronic states can be further simplified as shown in Figure 1D by introducing an effective intersystem crossing rate (k'_{isc}). The photoisomerization kinetics appears to occur with very fast time scales compared with the intersystem crossing kinetics ($k_{iso} \gg k_{isc}$) as explained later. Photoinduced

isomerization occurs in an ultrafast time scale if there is little or no potential energy surface between the singlet excited and partially twisted intermediate excited state of cyanine dye.¹⁵ The ultrafast isomerization is usually observed for a dye with a short methine bridge,¹⁶ such as the fluorophore studied here. If the rotation of the methine bridge is sufficiently hindered, then the isomerization of the fluorophore can be discernible with a 50 ns time resolution, and the quantum yield of the fluorophore is expected to be increased at least a few orders of magnitude in this case.

The fraction of the electronic states can be expressed with the rate constants discussed above by solving the linear differential equations according to simplified kinetic scheme (Figure 1D). Electron transition rate from S_1 to T is determined by effective intersystem crossing rate (k'_{isc}), which is an intersystem crossing rate multiplied by the scaling factor corresponding to the excited state fraction.

$$k'_{isc} = \frac{S_1}{S_0 + S_1 + P} k_{isc} \quad (2)$$

S and T denote singlet state and triplet state, respectively, of the dye ($S = S_0 + S_1 + P_0 + P_1$; $S + T = 1$). P_0 and P_1 indicate the ground and excited state of photoisomer, respectively. The fluorophore is assumed to be in the S_0 state before it is subject to the laser excitation with 514 nm wavelength, so that the initial conditions are $(S, T) = (1, 0)$ in the differential equations. The wavelength 514 nm is exactly matched with one of the two absorption maxima of the fluorophore.² Excited electrons on S_1 are deactivated by fluorescence, internal conversion, and isomerization, which are much faster processes than either of the processes of the intersystem crossing and triplet deactivation (k_{10} , k_{ic} , $k_{iso} \gg k'_{isc}$, k_T). Triplet state population of the fluorophores is usually balanced with the depopulation of the triplet state in a few microseconds time range.

By solving the differential equations, we get two eigenvalues, λ_1 and λ_2 , and two eigenequations, $S(t)$ and $T(t)$. $S(t)$ is the singlet state population ($S(t) = S_0 + S_1$), and $T(t)$ is the triplet state population. Two eigenvalues correspond to the average relaxation kinetic time. Assuming the excitation rate to be constant at time t , the probabilities of occupying different electronic states for the fluorophore at t as a function of t are given by

$$S(t) = \frac{k_T}{k'_{isc} + k_T} \exp(\lambda_1 t) + \frac{k'_{isc}}{k'_{isc} + k_T} \exp(\lambda_2 t) \quad (3)$$

$$T(t) = \frac{k'_{isc}}{k'_{isc} + k_T} \exp(\lambda_1 t) + \frac{k_T}{k'_{isc} + k_T} \exp(\lambda_2 t) \quad (4)$$

The eigenvalues λ_1 and λ_2 are related to the relaxation modes of the population kinetics of the two states and are given by

$$\lambda_1 = 0, \quad \lambda_2 = -(k_T + k'_{isc})$$

The first eigenvalue λ_1 is zero, demonstrating that the population of the singlet and triplet states eventually reaches a steady state as $t \rightarrow \infty$. The population of the triplet state, T_∞ , and its relaxation time, τ_∞ , at a steady equilibrium can be expressed as

$$T_\infty = \frac{k'_{isc}}{k'_{isc} + k_T} \quad (5)$$

$$\tau_\infty = \frac{1}{k'_{isc} + k_T} \quad (6)$$

This expression clearly shows us that the triplet state population can be dramatically increased if deactivation rate, k_T , is sufficiently small even though the cyanine dye has an extremely small intersystem crossing rate, k_{isc} .

The triplet state can be characterized by fitting the FCS curves with the well-known correlation function, as follows:

$$G(\tau) = G_D(\tau) \left[1 + \frac{T_\infty}{1 - T_\infty} \exp(-\tau/\tau_\infty) \right] \quad (7)$$

where $G_D(\tau)$ is the correlation function for the translational diffusion.

The oligodeoxyribonucleotide strands labeled with thiazole oranges, S' -d($T_6D_{514}T_6$)-3', were dissolved in glycerine and water mixture having viscosity of 2.5 cP at room temperature. At this point, transient dark state appearing around a few microseconds time range was assumed to be caused by the triplet state of the probe as it later proved to be reasonable. Figure 2 shows the effective intersystem crossing rate (k'_{isc}) and

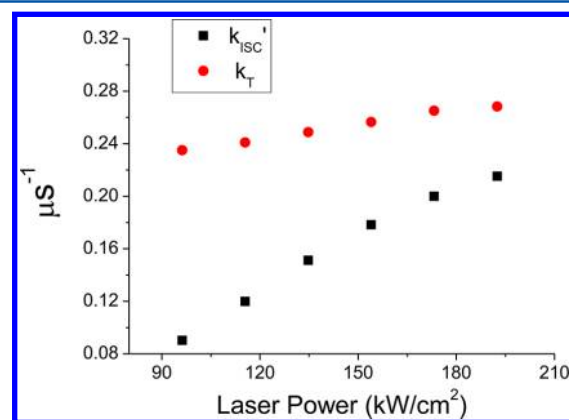


Figure 2. Fraction of triplet state versus the laser excitation intensity. The average laser power at the sample was adjusted to 80% laser transmission. The laser power with 80% transmission was 190 μ W (154 kW/cm²) at the output of an objective lens.

triplet state deactivation rate (k_T) plotted against the laser excitation intensity. The dramatic increase of the triplet state population is due to k'_{isc} increasing, while k_T remains constant along with excitation power. τ_∞ also decreased according to the excitation laser intensity as a result of the inversely linear relationship between τ_∞ and k'_{isc} .

Figure 3 shows the FCS curves with the addition of potassium iodide that were used to determine the population of the transient dark states and their relaxation times. In order to investigate the photodynamic features of the triplet state, potassium iodide was added in 0.5, 1.5, and 15 mM concentrations into the solution. The T_∞ and τ_∞ were observed to be 0.21 and 1.2 μ s, 0.19 and 0.6 μ s, and 0.15 and 0.08 μ s for the 0.5, 1.5, and 15 mM KI concentrations, respectively. It is well-known that iodide ion can act as an enhancer of intersystem crossing or quencher of triplet state.¹⁷ For a quencher of the triplet state, k'_{isc} may not be substantially changed, and k_T increases during the process of adding of the potassium iodine, which results in the behavior of T_∞ and τ_∞ . For an enhancer of intersystem crossing, the increase of T_∞ with a decrease of τ_∞ is expected, which is opposite to what

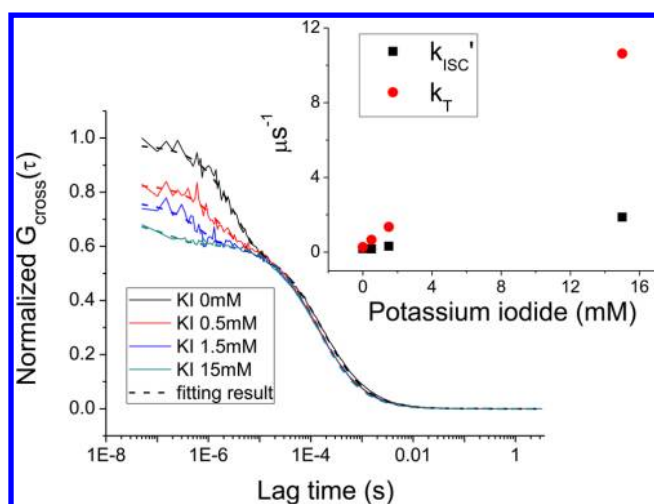


Figure 3. FCS curves of the sample with the addition of potassium iodide versus lag time. Transit time (τ_D) of each sample is 145 ± 6 , 146 ± 7 , and 152 ± 8 μ s for 0.5, 1.5, and 15 mM KI concentration, respectively.

occurred in this experiment. The triplet state can be quenched by a charge transfer since iodine ion acts as a weak electron donor¹⁸ even though the charge transfer state is not considered in Figure 1. The effect of the intersystem crossing caused by the heavy ion effects may be relatively small compared with the effect of the triplet deactivation rate in this experiment. Isomerization can be affected by ion pair formation between cationic dyes and dissolved anionic ions.^{19,20} Since the ion pairs between cationic dyes and counterions is known to form in the hydrophobic solvent, it is difficult to believe that the ionic pair is formed in this very hydrophilic solvent.

Figure 4 shows the FCS curves of the samples for the different solvent viscosity. In order to identify the viscosity

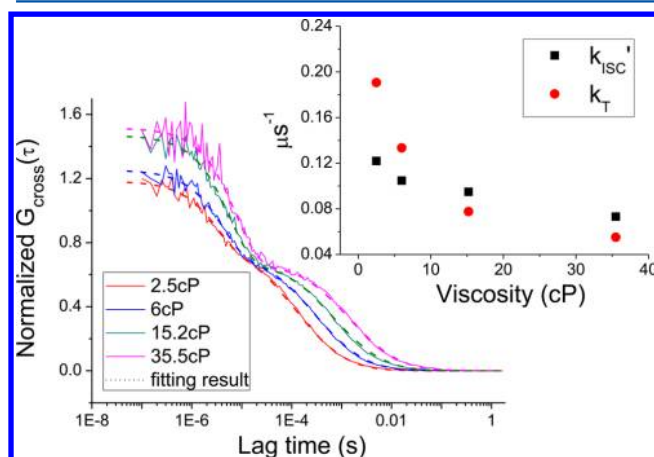


Figure 4. FCS curve of the sample at different solvent viscosity versus lag time. Transit time (τ_D) of each sample is 165 ± 6 , 372 ± 12 , 820 ± 21 , and 1747 ± 35 μ s for 2.5, 6, 15.2, and 35.5 cP, respectively.

dependence of the dark states, glycerin was added to the solution with solvent viscosities of 1, 2.5, 6, 15.2, and 35.5 cP. The population of the transient dark state and relaxation time increased simultaneously with increasing levels of viscosity. T_∞ and τ_∞ were observed to be 0.33 and 1.8 μ s, 0.39 and 3.2 μ s, 0.44 and 4.2 μ s, 0.55 and 5.8 μ s, and 0.57 and 7.8 μ s for 1, 2.5, 6, 15.2, and 35.5 cP, respectively. The increased hindrance of

the torsional rotation of the methine bridge led to an increase of the quantum yield of the fluorophore in the probe as indicated in Table 1. The increase of T_∞ can be explained by

Table 1. Fluorescence Quantum Yield of the Probe in Glycerine–Water Mixtures

solvent	quantum yield
glycerine 30% (2.5 cP)	0.031
glycerine 50% (6.0 cP)	0.043
glycerine 65% (15.3 cP)	0.060
glycerine 75% (35.5 cP)	0.095
after hybridization (2.5 cP)	0.580

the increase of k_{isc} or decrease of k_T . The increase of τ_∞ of the dark state can be explained by the decrease of k_T . Increases of both T_∞ and τ_∞ were possible only if the decrements of k_T , Δk_T , were larger than the increments of k_{isc} , Δk_{isc} . The triplet state can be quenched by the dissolved oxygen molecules with a charge transfer and/or energy transfer pathway.^{18,21,22} The importance of the spin statistical factor and diffusion-controlled rate is well-known for quenching the triplet state by oxygen molecules;²¹ the probability of the collisional interaction between the dye and oxygen is determined by the solvent viscosity and oxygen concentration. Furthermore, the increased viscosity can decrease the frequency of collisional quenching by the oxygen molecules. The oxygen concentration is decreased in a glycerin solution due to its low oxygen solubility. Therefore, a decrease in the collision rate between the oxygen molecules and the probe can lead to both an increase of the dark state fraction and an increase of the relaxation time. This is supported by the experiment with the oxygen scavenger, sodium sulfite, which is well-known for reducing the concentration of oxygen molecules dissolved in the solvent.²³

Figure 5 shows the FCS curves of the samples with the addition of oxygen scavengers. In order to identify the effect of the oxygen scavengers, sodium sulfite was added to the solution with concentration of 0, 1, and 2.5 mM, respectively. The T_∞ and τ_∞ were observed to be 0.42 and 2.3 μ s, 0.45 and 3.1 μ s,

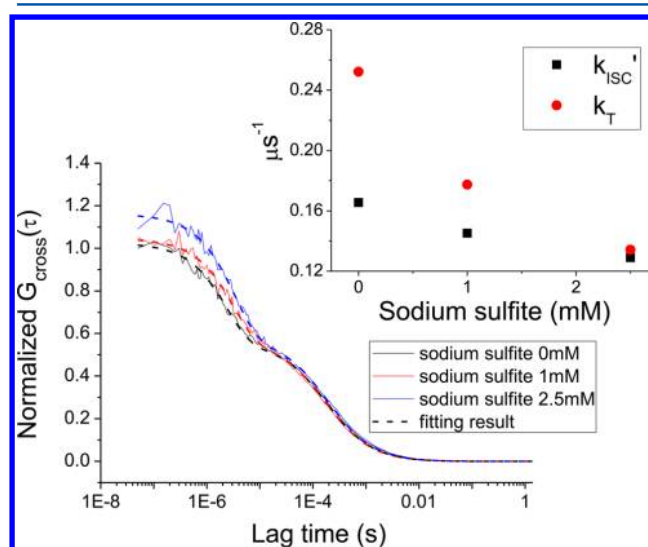


Figure 5. FCS curve of the sample with the addition of the sodium sulfite, oxygen scavenger, versus lag time. Transit time (τ_D) of each sample is 153 ± 4 , 160 ± 8 , and 165 ± 10 μ s for 0, 1, and 2.5 mM sodium sulfite, respectively.

and 0.49 and 3.8 μs for 0, 1, and 2.5 mM, respectively. The change in the correlation curves is well explained by the decrease in the oxygen concentration in the solvents. This verified that the decreased oxygen molecules are responsible for the increases of T_∞ and τ_∞ accompanied by a decrease of k_T .

Figure 6 shows the FCS curves before and after the hybridization of the DNA probe with the target DNA

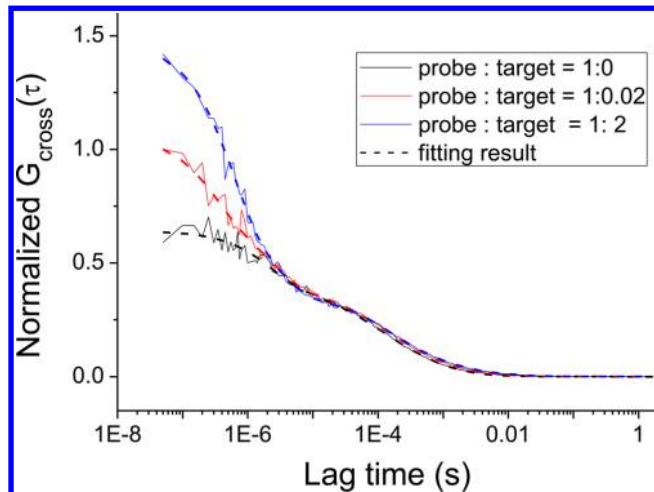


Figure 6. FCS curve of the sample with the addition of the target DNA versus lag time.

concentration. Before hybridization, the curve nicely fit into eq 7 with $T_\infty = 0.44$ and $\tau_\infty = 2.2 \mu\text{s}$. A dramatic increase of the dark state population was detected after the hybridization of the probe with even a small amount of target because the square of the probe brightness is directly multiplied to fluorescence correlation signals.²⁴ An increase of triplet state population and substantial decrease of its relaxation time are detected due to the relationship $\Delta k_{isc}' > \Delta k_T$ during the hybridization process. $\Delta k_{isc}'$ and Δk_T mean the change of the relaxation rate before and after the hybridization reaction. The increase of the S_1 population accompanied by the decreased k_{iso} enhances k_{isc}' , while the triplet state deactivation might be relatively insensitive to the hybridization. The intercalation of the dye into the DNA probe after the hybridization, which hinders the methine bridge rotation, is responsible for the fast to slow relaxation time scale. It is also noted that the time resolution of the ConfoCor 3 spectrometer used in this experiment is 50 ns. The hindrance of the photoisomerization and the increase of the quantum yield of the fluorophore in the DNA probe were clearly observed (Table 1). The FCS curve obtained after the hybridization failed to fit eq 7 only, but the introduction of a new multiplicative factor into eq 7 can fit the experimental data well since the samples containing a target make a multi-component decay in FCS. It is not easy to obtain reasonable deconvolution results in these experimental results since the two components coming from bound probe and nonbound probe are largely overlapped in FCS signal. In addition, the isomerization process may appear in a detectable time range of our experimental resolution since isomerization of the probe is significantly retarded after hybridization. This result, however, can be useful for the probe/target complex characterization in cell experiments. For instance, the fluorescence detection/imaging techniques for mRNA in a live cell have difficulty in cell experiments because the target DNA/RNA detection is largely interrupted by background such as scattered excitation

light, autofluorescence, and fluorescence of free probes. Therefore, these techniques require a complicated tag technology²⁵ or artificially target-enriched cell.²⁶ If we use the transient dark state (i.e., triplet state) in target detection, we can improve these problems because the scattered light or autofluorescence would not give a specific change on the dark state in FCS. The interference originated from uncorrelated signal can be eliminated through fluorescence correlation measurement, and the change of the probe's dark state is distinctive to the uncorrelated signal originated from the cell organelle. The triplet state appeared in FCS is highly sensitive and specific to the change of environment, such as viscosity, quencher, and target molecule concentration.

Transient dark state caused by isomerization is determined by effective isomerization rate (k_{iso}') and effective back-isomerization rate (k_{biso}'). The change of its population fraction is relatively small because both of the isomerization and back-isomerization rates are increased or decreased simultaneously according to the factors that influence the rotation of the methine bridge. Therefore, it is a reasonable assumption that the dark state caused by isomerization may be relatively insensitive to the environment (viscosity, target, etc.). By the way, the fraction of the triplet state is determined by the effective intersystem crossing rate (k_{isc}') and triplet deactivation rate (k_T). It is also a reasonable assumption that the triplet deactivation rate (k_T) is insensitive compared to the effective intersystem crossing rate (k_{isc}') in the change of methine bridge hindrance. The change of isomerization directly affects the effective intersystem crossing rate, while the triplet state deactivation is weakly related to the rotation of the methine bridge. Therefore, we can assume that the triplet dark state would be more sensitive to the ambient chemical or physical conditions (viscosity, triplet state quencher, and target) compared to that of an isomer state, and this can be used as a sensitive indicator to the environmental changes.

In this report, we demonstrate the transient dark state of hybridization-sensitive DNA/RNA probe and suggest that the conventional visualization of fluorescence intensity based DNA/RNA in living cells can be facilitated by FCS, which can provide other useful parameters such as concentration, diffusion, and interactions for target RNAs. Interestingly, the triplet dark state of D_{514} is very sensitively changed by the presence of the target DNA. In FCS, triplet state relaxation occurred in a distinctive time range before and after hybridization. By using this time-resolved fluorescence detection as well as diffusion, we can increase the detection contrast before and after hybridization in living cells as well as in vitro. A detailed quantitative study of hybridization through FCS along with conventional fluorescence intensity analysis in such conditions with various D_{nm} probes will be reported in a forthcoming paper.

CONCLUSIONS

The triplet state of the hybridization-sensitive DNA probe, which has been developed for RNA visualization in live cells, was investigated using fluorescence correlation spectroscopy. The dark state decreased with the addition of potassium iodide in the samples. The triplet state can be quenched using iodine ion through a charge transfer reaction. The simultaneous increase of the dark state population and relaxation time according to the solvent viscosity was also detected. The triplet state appears to be efficiently quenched by the oxygen molecules, which was further supported by the experiments

with oxygen scavengers. The two state model developed in this study can provide a reasonable explanation for most of these experimental results. The transient dark state population observed in a time scale of a few microseconds was dramatically increased through the hybridization with the target DNA. The additional dark states, which could be ascribed to the triplet state and isomerized state of hybridized probe, appear in a distinctive time scale after the hybridization reaction

AUTHOR INFORMATION

Corresponding Author

*E-mail: sykim@kaist.ac.kr (S.Y.K.); cback@riken.jp (C.-G.P.).

Notes

The authors declare no competing financial interest.

ACKNOWLEDGMENTS

We are thankful to the unknown referees' fruitful comments. This research was supported by the Basic Science Research Program through the National Research Foundation of Korea (NRF) funded by the Ministry of Education, Science and Technology (R0A-2007-000-20052-0). It was supported through the RDA Agenda Project and General Individual Research Program from National Research Foundation of Korea (NRF). We thank the 'Korean Basic Science Institute (KBSI)' for allowing the use of their ConfoCor 3 spectrometer for the measurement of the fluorescence correlation spectrum of the samples

REFERENCES

- (1) Ikeda, S.; Okamoto, A. *Chem. Asian J.* **2008**, *3*, 958–968.
- (2) Shin, H. S.; Okamoto, A.; Sako, Y.; Kim, S. W.; Kim, S. Y.; Pack, C. G. *J. Lumin.* **2012**, *132*, 2566–2571.
- (3) Okamoto, A. *Chem. Soc. Rev.* **2011**, *40*, 5815–5828.
- (4) Kubota, T.; Ikeda, S.; Okamoto, A. *Bull. Chem. Soc. Jpn.* **2009**, *82*, 110–117.
- (5) Pack, C.; Saito, K.; Tamura, M.; Kinjo, M. *Biophys. J.* **2006**, *91*, 3921–3936.
- (6) Widengren, J.; Schwille, P. *J. Phys. Chem. A* **2000**, *104*, 6416–6428.
- (7) Yeh, H. C.; Puleo, C. M.; Ho, Y. P.; Bailey, V. J.; Lim, T. C.; Liu, K.; Wang, T. H. *Biophys. J.* **2008**, *95*, 729–737.
- (8) Chibisov, A. K. *High Energy Chem.* **2007**, *41*, 200–209.
- (9) Webster, S.; Padilha, L. A.; Przhonska, O. V.; Pecelil, D.; Hu, H.; Slominsky, Y. L.; Kachkovski, A. D.; Tolmachev, A. I.; Kurdyukov, V. V.; Hagan, D. J.; Van Stryland, E. W. Enhancement of Triplet Yields in Cyanine-Like Molecules. In *Laser Science XXV*; Optical Society of America: San Jose, CA, 2009.
- (10) Widengren, J.; Rigler, R.; Mets, U. *J. Fluoresc.* **1994**, *4*, 255–258.
- (11) Widengren, J.; Mets, U.; Rigler, R. *J. Phys. Chem.* **1995**, *99*, 13368–13379.
- (12) Ikeda, S.; Kubota, T.; Yuki, M.; Okamoto, A. *Angew. Chem., Int. Ed.* **2009**, *48*, 6480–6484.
- (13) Dempster, D. N.; Morrow, T.; Rankin, R.; Thompson, G. F. *J. Chem. Soc., Faraday Trans.* **1971**, *68*, 1479.
- (14) Kasha, M.; Rawls, H. R.; El-Bayoumi, M. A. *Pure. Appl. Chem.* **1965**, *11*, 371–392.
- (15) Sanchez-Galvez, A.; Hunt, P.; Robb, M. A.; Olivucci, M.; Vreven, T.; Schlegel, H. B. *J. Am. Chem. Soc.* **2000**, *122*, 2911–2924.
- (16) Dietzek, B.; Yartsev, A.; Tarnovsky, A. N. *J. Phys. Chem. B* **2007**, *111*, 4520–4526.
- (17) Chmyrov, A.; Sandén, T.; Widengren, J. *J. Phys. Chem. B* **2010**, *114*, 11282–11291.
- (18) Chibisov, A. K. *J. Photochem.* **1976**, *6*, 199–214.
- (19) Ishchenko, A. A. *Russ. Chem. Rev.* **1991**, *60*, 865–884.
- (20) Tatikolov, A. S.; Dzhalibekov, K. S.; Shvedova, L. A.; Kuzmin, V. A.; Ishchenko, A. A. *J. Phys. Chem.* **1995**, *99*, 6525–6529.
- (21) Garner, A.; Wilkinson, F. *Chem. Phys. Lett.* **1977**, *45*, 432–435.
- (22) Wilkinson, F.; Abdel-Shafi, A. A. *J. Phys. Chem. A* **1999**, *103*, 5425–5435.
- (23) Wang, L.; Zhao, Y. *Chem. Eng. J.* **2008**, *136*, 221–226.
- (24) Lakowicz, J. R. *Principles of Fluorescence Spectroscopy*, 3rd ed.; Springer: New York, 2006.
- (25) Kubota, T.; Ikeda, S.; Yanagisawa, H.; Yuki, M.; Okamoto, A. *PLoS One* **2010**, *5*, e13003.
- (26) Okamoto, A. *Chem. Soc. Rev.* **2011**, *40*, 5815–5828.